The Journal of Agricultural Science

cambridge.org/ags

Climate Change and Agriculture Research Paper

Cite this article: Fang G, Chen Y, Li Z (2018). Variation in agricultural water demand and its attributions in the arid Tarim River Basin. *The Journal of Agricultural Science* **156**, 301–311. https://doi.org/10.1017/S0021859618000357

Received: 22 September 2017
Revised: 1 April 2018
Accepted: 25 April 2018
First published online: 21 May 2018

Key words:
Attribution analysis; Climate change; Crop water requirement; Evapotranspiration; Penman–Monteith

Author for correspondence:
Y. Chen, E-mail: chenyn@ms.xjb.ac.cn

Variation in agricultural water demand and its attributions in the arid Tarim River Basin

G. Fang[1,2], Y. Chen[1] and Z. Li[1]

[1]State Key Laboratory of Desert and Oasis Ecology, Xinjiang Institute of Ecology and Geography, Chinese Academy of Sciences, 830011 Urumqi, China and [2]Department of Geography, Ghent University, 9000 Ghent, Belgium

Abstract

Agricultural water use accounts for more than 95% of the total water consumption in the extreme arid region of the Tarim River Basin. Understanding the variation of agricultural water demand (*AWD*) and its attributions is therefore vital for irrigation management and water resource allocation affecting the economy and natural ecosystems in this high water-deficit region. Here spatial–temporal variations of *AWD* based on weighted crop water requirement (ET_c) were estimated using the Penman–Monteith equation and the crop coefficient approach. Then the contributions of meteorological factors and planting structure (i.e. proportions of crop acreages) to *AWD* variations were quantified based on traditional methods and numerical experiment (i.e. a series calculation of *AWD* based on different input data). Results indicated that *AWD* decreased during 1960–1988 at a rate of 2.76 mm/year and then started to increase at a high rate of 9.47 mm/year during 1989–2015. For the first period (1960–1988), wind speed (*uz*), maximum humidity (RH_{max}) and sunshine duration (*n*) were the most important factors leading to decreased *AWD*, while for the second period the evolution of planting structure was the most significant factor resulting in the rapid increase of *AWD*, followed by the minimum temperature (T_{min}), *uz* and RH_{max}. The evolution of planting structure alone would lead to an increase rate for *AWD* of 7.1 mm/year while the climatic factor would result in an increase rate of 1.9 mm/year during 1989–2015.

Introduction

The Tarim River basin, located in the mid-latitude and extremely arid region of the northern hemisphere, has experienced the most prominent warming during the past few decades (Chen *et al*., 2009; Li *et al*., 2017*b*). Characterized by scarce water resources and a fragile ecological system, this region is strongly affected by climate change (Chen, 2015), which has intensified agricultural water consumption and exacerbated the already-serious water crisis.

During recent decades, with global warming and rapid increase in the use of irrigation water, ecological water has been seriously squeezed out, causing large areas of desert vegetation to die (Chen *et al*., 2016). To alleviate deterioration of the ecological environment and promote socio-economic development in the Tarim River Basin, the State Council of the People's Republic of China formally approved the 'Comprehensive management report of the Tarim River Basin' in June 2001 (Chen *et al*., 2017). The government invested 10.7 billion Renminbi (RMB) to strengthen management of the river basin, focusing on water saving in the irrigation area, including reconstruction of plain reservoirs, groundwater exploitation and utilization, ecological reconstruction and construction of mountain reservoirs (Chen *et al*., 2017). However, land reclamation increased rapidly with more and more high water-consuming crops (e.g. cotton, fruit trees, etc.) being grown during recent decades. The cultivated land was only 13 093 km^2 in 1949, increasing to 35 428 km^2 in 2000 and 42 292 km^2 in 2010 (Chen, 2015). According to the Xinjiang Statistical Yearbooks 1989–2016 (Statistical Bureau of Xinjiang Uygur Autonomous Region, 1989–2016), the proportion of cotton acreage has also increased from 0.16 in 1988 to 0.44 in 2015. With the rapid growth in population and agricultural land, water shortage has become a major limiting factor for the socioeconomic development in the Tarim River Basin (Shen *et al*., 2013).

Recently, many previous studies have investigated variations of reference evapotranspiration (ET_0) and crop water requirement (*ETc*) and their responses to climate change (Rodríguez Díaz *et al*., 2007; Mo *et al*., 2009; Liang *et al*., 2011; Shen *et al*., 2013; Tabari and Talaee, 2014; Fan *et al*., 2016). It is normally recognized that higher than normal temperatures were the cause of increased evaporation, as air warming will enhance the atmospheric water vapour deficit and the slope of vapour saturation to temperature (Li *et al*., 2014, 2017*b*). Yet, there is evidence that the direct impact of temperature on increased *ETc* may be a misinterpretation. As is argued by Acharjee *et al*. (2017), a warming climate does not always result in higher agricultural water use, as the combined effects of wind speed, humidity and sunshine hours are closely related (Sherwood and Fu 2014; Li *et al*., 2017*b*). Gao *et al*. (2006) and Fan *et al*. (2016) found that the declining tendencies of sunshine duration (n) and/or wind speed (uz) were major causes for the negative trend of ET_0 in most areas of China. Similar results were also obtained in studies suggesting that variations of uz and net radiation could be the major factors influencing variation in ET_0 (Yin *et al.*, 2008; Fan *et al.*, 2016; Li *et al.*, 2017*a*).

However, few studies have investigated regional agricultural water demand (*AWD*) variation in the arid regions and contributing factors. Döll (2002) estimated that two-thirds of the global area equipped for irrigation in 1995 would possibly suffer from increased water requirements; Shen *et al.* (2013) indicated that the rapid increase in cotton cultivation area resulted in a swift increase in irrigation water requirement in north-western China. As agricultural water consumption accounts for 95% of total water use in the Tarim River Basin, *AWD* changes will exert a significant impact on water demand. Quantifying the contribution of each factor (related to both climate change and human activity) to *AWD* is of great significance to help improve water management toward sustainable water use.

In the current study, the Penman–Monteith equation (Allen *et al.*, 1998) and crop coefficient approach together with the weighted average method were applied to estimate *ETc* and *AWD* in the Tarim River Basin. To understand the main factors contributing to changes in *AWD*, traditional contribution method and numerical experiments were designed. Questions addressed include the following: (1) How did the *ETc* and *AWD* change in the Tarim River basin during 1960–2015? (2) What were the main factors influencing *AWD* evolution? (3) What is the role of planting structure (i.e. proportion of crop acreage) in *AWD* variation? Understanding these issues will provide information to the policymakers in terms of adaption of water scarcity intensified by climate change.

Methodology

Study area and data

The Tarim River Basin, with a drainage area of 1 020 000 km^2, is surrounded by the Tienshan Mountains in the north and the Kunlun Mountains in the south with large areas of alpine, inland basin and widespread desert. This region has a continental climate, with little rainfall throughout the year and strong evaporative potential. The average annual precipitation is estimated to be 200 mm in the alpine area but only 20 mm in the sandy desert. Annual precipitation is generally <50 mm in the oasis areas, where most agricultural activities exist (Fig. 1). However, potential evaporation in this arid region can be as large as 3200 mm/year, 8–10 times the annual rainfall (Shen and Chen, 2010; Chen *et al.*, 2011), making this area one of the most arid regions in the world (Shen and Chen, 2010; Shen *et al.*, 2013). The arable land is mainly distributed in oases embedded at the edge of the deserts, relying on surface water and groundwater for irrigation.

Daily meteorological data were derived from the China Meteorological Administration (CMA, http://data.cma.cn/). This dataset was compiled through preliminary automated quality control and has been widely used in climate change related studies (Liu *et al.*, 2004; Zhai *et al.*, 2005). Taking into account data availability and reliability, meteorological variables including the maximum, mean and minimum temperature (abbreviated hereafter as $T_{\max}$, T_a and $T_{\min}$), wind speed (uz), sunshine duration (n), and maximum and minimum relative humidity ($RH_{\max}$ and $RH_{\min}$) from 1960 to 2015 at 24 stations were used to calculate ET_0 and *AWD* (Table 1). Most stations are located in the oasis area of the Tarim River Basin (Fig. 1).

Calculation of reference evapotranspiration, crop water requirement and agricultural water demand

Figure 2 shows the calculation for the basin-scale *AWD* influenced by climate change and human activity. The Penman–Monteith approach, recommended by the UN Food and Agriculture Organization (FAO), was used to estimate ET_0 as it is widely recognized as being effective and efficient in calculating ET_0 (Allen *et al.*, 1998; Shen *et al.*, 2013). Reference evapotranspiration was defined and calculated based on the evapotranspiration of well-watered short grass of 0.12 m in height, resistance of 70 s/m and albedo of 0.23 (Allen *et al.*, 2005):

$$ET_0 = \frac{0{\cdot}408\Delta(R_n - G) + \gamma\frac{900}{T_a + 273}u_2(e_s - e_a)}{\Delta + \gamma(1 + 0{\cdot}34u_2)} \qquad (1)$$

where R_n (MJ/(m^2/day)) is the net daily radiation at the vegetation surface and the calculation of R_n is dependent on sunshine hours (n) (measured at a meteoroogical station), as illustrated in McMahon *et al.* (2013); G (MJ/(m^2/day)) is the soil heat flux, which is generally assumed to be negligible for daily time-steps; u_2 (m/s) is the average daily wind speed at 2 m height observed at each meteorological station; e_s (kPa) is saturation vapour pressure expressed as a function of measured $T_{\max}$ and $T_{\min}$; e_a (kPa) is mean daily actual vapour pressure calculated using measured $T_{\max}$, $T_{\min}$, $RH_{\max}$ and $RH_{\min}$; Δ(kPa/°C) is the slope of the saturation vapour pressure curve, which is a function of observed mean daily temperature; and γ (kPa/°C) is the psychrometric constant. The detailed computation methods for these variables are given in McMahon *et al.* (2013). The R-package 'Evapotranspiration' was applied to calculate ET_0 at each meteorological station on a daily basis (Guo *et al.*, 2016).

The *ETc* of each crop at station j was calculated based on the crop coefficient approach (Eqn 2).

$$ETc_{i,j} = K_{ci} \times ET_{0j} \qquad (2)$$

where $ETc_{i,j}$ (mm) and K_{ci} (-) are the crop water requirement and crop coefficient for the ith crop at station j. The controlling area of station j was defined by Thiessen polygon division (Fig. 3*a*). The K_c value reflects the crop's relative water consumption capacity during different growing stages. It includes three parts: basal crop coefficient, the evaporative component of the bare soil fraction and the water stress coefficient (Calera *et al.*, 2017), and serves as an aggregation of the physical and physiological differences between a certain crop and the reference crop. In the current study, the five major crops covering the largest planting area, i.e. cotton, wheat, maize, rice and fruit trees, were considered. Other crops, including beet, potato, soybean, vegetable, oilseed rape and peanut, were not separately recorded due to their small planting areas (<0.16). Crop coefficients of cotton, wheat, maize, rice and fruit trees were derived from FAO recommendations (Allen *et al.*, 1998) and previous studies (Zhang *et al.*, 2010; Wang *et al.*, 2015). The intra-annual variations of K_c values are shown in Fig. 3*b*.

AWD was a weighted average of $ETc_{i,j}$:

$$AWD = \sum_{i=1}^{N}(ETc_{i,j} \times f_i) \qquad (3)$$

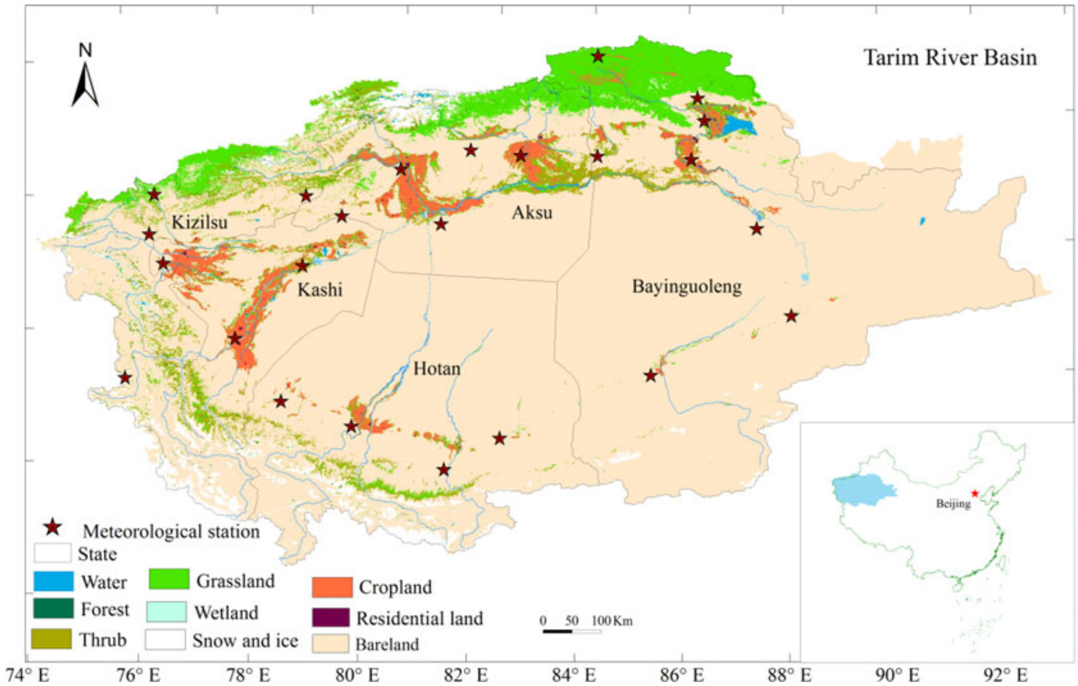

Fig. 1. The location and landuse map of the Tarim River Basin together with the meteorological stations.

where f_i is the proportion of planting area for crop i and N is number of crop types ($N = 5$ in this case). Since the planting structure is only available for the five autonomous prefectures or states (i.e. Bayinguoleng, Aksu, Kizilsu, Kashi, Hotan), the area (proportion) of each crop f_i at each Thiessen polygon was assumed to be the same as its closest state.

A quantitative indicator, K_{cw} (i.e. weighted crop coefficient), was defined to represent quantitatively the impact of changings planting structures on regional water demand. It increases with the increase in area proportion of high water consuming crops:

$$K_{cw} = \sum_{i=1}^{N} (Kc_i \times f_i) \tag{4}$$

Traditional contribution analysis

The widely used contribution analysis (to differentiate it from the following numerical experiments, this method was referred to as ‘traditional analysis’) was applied to quantify the contribution of each meteorological factor and planting structure factor to *AWD* variation. The contribution index was defined by multiplying the response of *AWD* to a single factor by its relative change rate (McCuen, 1974; Li *et al.*, 2017*a*):

$$S_{Vi} = \lim_{\Delta \to 0} \left(\frac{\Delta AWD/AWD}{\Delta V_i / V_i} \right) = \frac{\delta AWD}{\delta V_i} \frac{V_i}{AWD} \tag{5}$$

$$\mathrm{Con}_{Vi,r} = S_{Vi} \times \frac{L \times Trend_{Vi}}{|\overline{Vi}|} \times 100 \tag{6}$$

where S_{Vi} is a unitless index meaing the response of *AWD* (mm) to factor *Vi*; $\mathrm{Con}_{Vi,r}$ (%) is the contribution of a driving factor V_i to *AWD* variation; L is the number of years in one period. $Trend_{Vi}$ and $|\overline{V_i}|$ are the annual trend and absolute mean value of V_i; and ΔAWD and ΔV_i are the variations of *AWD* and V_i. If the contribution rate $\mathrm{Con}_{Vi,r} > 0$, then the factor variation promotes *AWD* increase, and vice versa. The higher the absolute value of $\mathrm{Con}_{Vi,r}$, the greater contribution of factor V_i.

Numerical experiment in contribution analysis

To disentangle different responses of *AWD* to forcing factors, several numerical experiments were designed to examine the *AWD* variation when the specific factors were free of any trends. To do that, a ‘Detrending’ approach was applied to remove the trends in these forcing factors.

Several numerical experiments were designed: (a) $T_{\max}$ *case* (detrending all variables except $T_{\max}$); (b) $T_{\min}$ *case* (detrending all variables except $T_{\min}$); (c) *uz case* (detrending all variables except *uz*); (d) *n case* (detrending all variables except *n*); (e) $RH_{\max}$ *case* (detrending all variables except $RH_{\max}$); (f) $RH_{\min}$ *case* (detrending all variables except $RH_{\min}$); (g) K_{cw} *case* (detrending all the meteorological factors but K_{cw}); (h) *base case* (detrending all forcing factors). The trends in *AWD* calculated from these experiments were compared with each other.

The simple and widely used ‘Detrending’ approach could eliminate the linear trend from the original meteorological variable (Zhang *et al.*, 2016; Li *et al.*, 2017*b*). Equation (7) illustrates how to remove the trends in variable $T_{\max}$ and $T_{\min}$:

$$T_{\mathrm{detrend,yr}} = T_{\mathrm{observed,yr}} - \beta(\mathrm{yr}_{\mathrm{order}} - 1960) \tag{7}$$

where $T_{\mathrm{detrend,yr}}$ (°C) and $T_{\mathrm{observed,yr}}$ (°C) are the detrended and observed annual values, and β (°C/year) is the annual trend of $T_{\max}$ or $T_{\min}$ estimated based on least squares. $\mathrm{yr}_{\mathrm{order}}$ denotes the year 1960, 1961,…, 2015.

For other meteorological factors and planting factor K_{cw}, the Sen’s slope estimator (Sen, 1968) was used to determine the

Table 1. Information of the meteorological stations in the Tarim River Basin and the average annual reference evapotranspiration (ET_0)

Station no.	Name	Longitude (°)	Latitude (°)	Elevation (m a.s.l.)	ET_0 (mm)
51467	Baluntai	86.20	42.40	1740	1035.5
51542	Bayanblak	84.09	43.02	2439	744.9
51567	Yanqi	86.34	42.05	1058	1096.5
51628	Aksu	80.14	41.1	1105	1078.7
51633	Baicheng	81.54	41.47	1230	903.8
51642	Luntai	84.15	41.47	978	1078.0
51644	Kuche	82.57	41.43	1082	1224.8
51656	Korla	86.08	41.45	933	1308.3
51701	Turgat	75.24	40.31	3507	796.6
51705	Wuqia	75.15	39.43	2178	1187.7
51709	Kashi	75.59	39.28	1289	1214.1
51711	Aheqi	78.27	40.56	1986	1126.6
51716	Bachu	78.34	39.48	1117	1176.9
51720	Keping	79.03	40.30	1163	1168.8
51730	Alaer	81.03	40.30	1013	1133.8
51765	Tieganlik	87.42	40.38	846	1265.2
51777	Ruoqiang	88.10	39.02	888	1435.5
51804	Tashi	75.14	37.47	3090	1071.3
51811	Shache	77.16	38.26	1231	1156.8
51818	Pishan	78.17	37.37	1376	1155.3
51828	Hotan	79.56	37.08	1375	1266.7
51839	Minfeng	82.43	37.04	1411	1210.1
51855	Qiemo	85.33	38.09	1248	1247.8
51931	Yutian	81.39	36.51	1423	1154.2

magnitude of change over time series. The Sen's slope method is a non-parametric method (Sen, 1968) quantifying the linear median (50th percentile) concentration changes with time and is used to determine the magnitude of the trend line:

$$Q_j = \frac{X_r - X_k}{r - k}, \text{ for } j = 1, \ldots, N;\ k < r < M \quad (8)$$

where X_r and X_k are the data values at time r and time k, respectively. Normally, $N = M(M-1)/2$, where M is the length of data series. The Sen's slope β is then estimated as the median value of Q_j. The trends in annual series were firstly removed by Eqn (9):

$$F_{y\text{-detrend,yr}} = F_{y\text{-observed,yr}} - \beta(\text{yr}_{\text{order}} - 1960) \quad (9)$$

where $F_{y\text{-detrend,yr}}$ is the detrended annual value of Vi in year yr and $F_{y\text{-observed,yr}}$ is original (i.e. observed) annual value in the same year. $F_{y\text{-detrend,yr}}$ and $F_{y\text{-observed,yr}}$ have the same units as

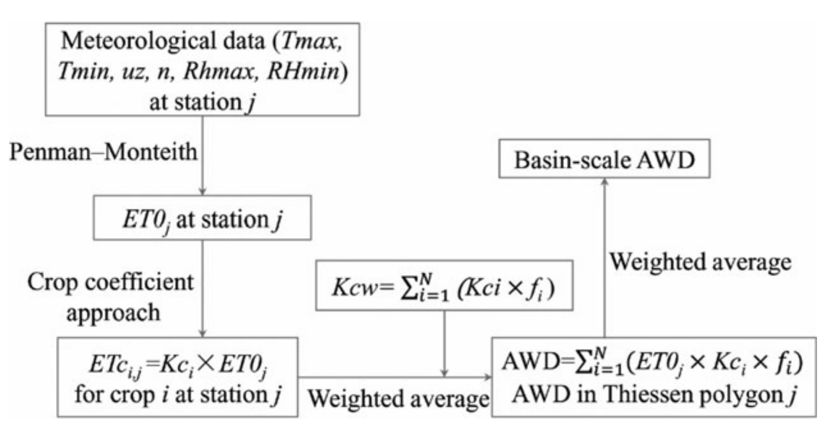

Fig. 2. Calculation procedure for the basin-scale agricultural water demand (*AWD*). The climate variables include maximum temperature (T_{max}), minimum temperature (T_{min}), wind speed (uz), sunshine hours (n), maximum relative humidity (RH_{max}), minimum relative humidity (RH_{min}). Human activity (planting structure factor) is represented by K_{cw}.

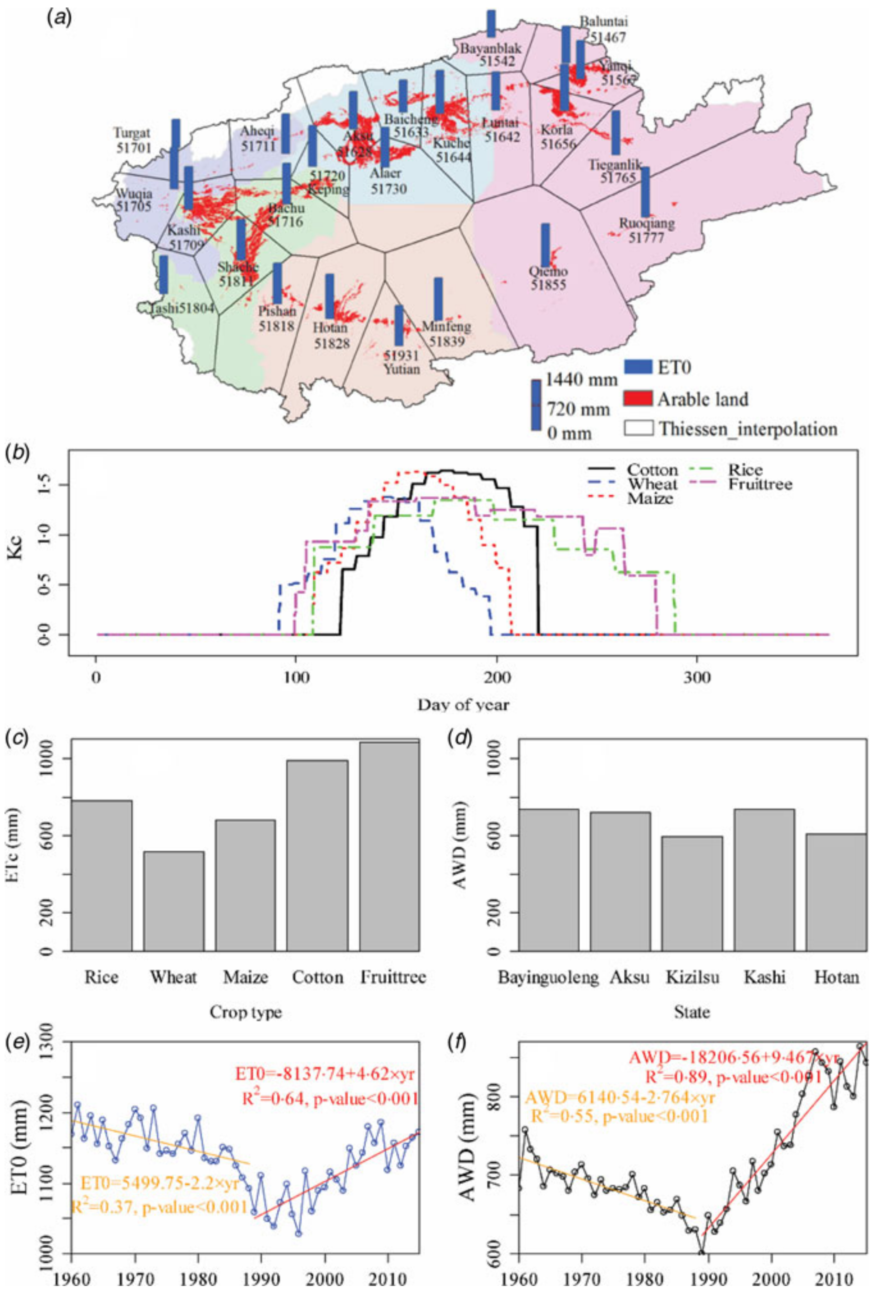

Fig. 3. (*a*) Thiessen polygon division and the spatial variation of average annual reference evapotranspiration (ET_0) during 1960–2015. The red patches represent the farmland distribution with the light background indicating different states. (*b*) The intra-annual variations of crop coefficient during different growing stages (K_c) of main crops in the Tarim River Basin. (*c*) Crop water requirement (*ETc*) of different crops based on ET_0 data at the Kashi meteorological station, which controls the largest irrigation area in the Tarim River Basin. (*d*) Agricultural water demand (*AWD*) for each state. (*e*) Variation of basin-averaged ET_0 and (*f*) Variation of basin-scale agricultural water demand (*AWD*) during 1960–2015.

the target variable V_i. β (mm/yr for *AWD*, hour/year for *n*, *etc*) is the annual trend of *Vi* estimated using Sen's slope method. Then the annual ratio was applied to the daily timescale to generate a daily time series:

$$F_{\mathrm{detrend},d} = F_{\mathrm{observed},d} \times \frac{F_{y\text{-detrend},\mathrm{yr}}}{F_{y\text{-observed},\mathrm{yr}}} \quad (10)$$

where $F_{\mathrm{detrend},d}$ and $F_{\mathrm{observed},d}$ are the detrended and observed daily values at day d in year yr. As with $F_{y\text{-detrend},\mathrm{yr}}$ and $F_{y\text{-observed},\mathrm{yr}}$, $F_{\mathrm{detrend},d}$ and $F_{\mathrm{observed},d}$ have the same units as the target variable V_i.

Finally, the detrended and observed variables were combined to generate *AWD*. To understand the influence level of each forcing factor on *AWD*, $\mathrm{Con}_{Vi,e}$ was applied to measure the contributions from different factors to *AWD* variation:

$$\mathrm{Con}_{Vi,e} = \frac{\delta AWD}{\delta V_i}\frac{\delta V_i}{t} \quad (11)$$

where $\mathrm{Con}_{Vi,e}$ (mm/yr) is the contribution of factor V_i to *AWD* variation based on the numerical experiments.

Results

Spatial–temporal variations of reference evapotranspiration and agricultural water demand

Daily ET_0 at 24 stations were calculated and the distribution map of their mean annual values during 1960–2015 is displayed in Fig. 3*a*. The average ET_0 of these 24 stations was estimated to be 1163 mm, ranging from 796.6 to 1435.5 mm. Areas with large ET_0 were mainly distributed in low altitude regions, while low ET_0 values occurred mainly in high altitude regions (e.g. Bayanbulak51542, Baicheng51633, Turgat51701 and Tashi51804).

Figures 3*c* and 3*d* show the crop water requirements (ET_c) of different crops at the Kashi station and regional *AWD* for the five states. Fruit trees had the highest ET_c, approaching 1084.5 mm, followed by cotton (987.2 mm) and rice (778.9 mm), while ET_c of wheat was the lowest (514.8 mm). Regionally, the *AWD* was estimated for each state. The highest *AWD* occurred in Bayinguoleng, and Kizilsu had the lowest *AWD*/m^2. The time series of basin-averaged ET_0 and *AWD* during 1960–2015 are shown in Fig. 3. A turning point (year 1988) was detected based on Student's *t* method. The ET_0 demonstrated a decreasing trend during 1960–1988 (decreasing rate = 2.20 mm/yr) and then started to increase from 1989 (increasing rate = 4.62 mm/year). Agricultural water demand had a similar pattern to that of ET_0, with a turning point detected in 1988. It is worth noting that *AWD* has increased since 1989 at a very high rate of 9.47 mm/year. By 2010–2015, the *AWD* in the study region reached up to 826.1 mm/year. This represented a 16.4% increase from 683.7 mm/year during 1960–1988 to 795.9 mm/year since the beginning of the 21st century.

The variations of meteorological factors in the Tarim River Basin are shown in Fig. 4. T_{max} and T_{min} showed continuous increasing trends, with annual increases of 0.019 and 0.039 °C/year, respectively. *uz* and *n* show similar patterns of variation to ET_0 and *AWD*, which decreased over the period of 1960–1988 and then increased over 1989–2015. Meanwhile, RH_{max} and RH_{min} demonstrated substantial decreasing trends of 0.145 and 0.179%/year, respectively, since 1989. All the meteorological factors examined showed obvious increasing or decreasing trends, which favoured the increase of ET_0 and *AWD* during 1989–2015.

The proportions of crop acreages also changed since the 1980s, with an obvious decrease in wheat ratio (proportion of wheat area to agricultural acreage) and increasing ratios of cotton and fruit trees (proportions of cotton area and fruit tree area). As crop area data are not available before 1988, it was assumed that planting area during 1960–1988 was the same as that in 1988, which may not have been the case. The proportions of areas growing low-water-consuming crops (e.g. wheat, maize) exhibited a continuous decreasing trend, while high-water-consuming crops (e.g. cotton, fruit trees) have been increasing since 1988. The proportion of crop area given to fruit trees increased substantially from 8.15% during 1989–2000 to 29% by 2010 and then decreased slightly to 21.1% by 2015. The increases of crops with high water consumption led to increased K_{cw}, especially for Bayinguoleng state (Fig. 4).

Quantifying the contributions of agricultural water demand variation

As the *AWD* showed an inverse trend during 1989–2015 compared with 1960–1988, the *AWD* variations during 1960–1988 and 1989–2015 were investigated. For each time period, the

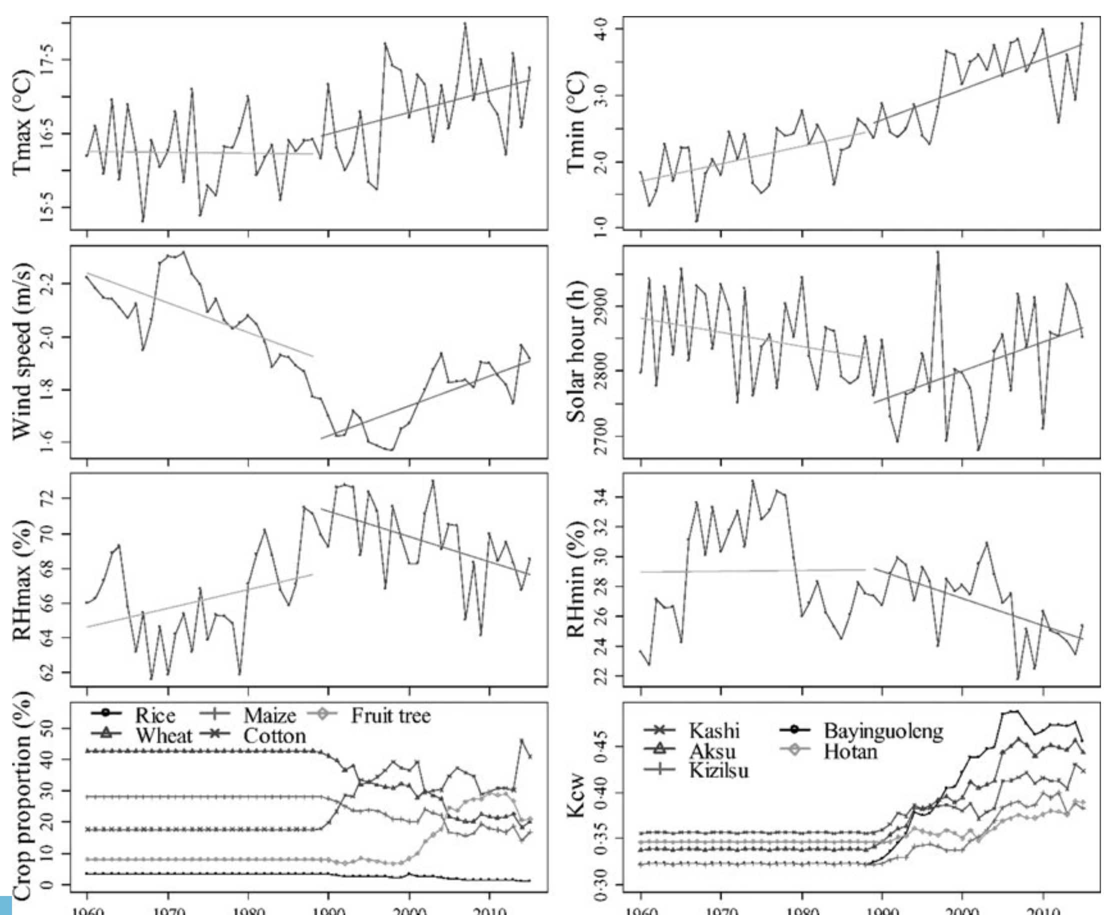

Fig. 4. Variations of the meteorological variables and planting structure factor (K_{cw}) in the Tarim River Basin.

Table 2. Contributions of meteorological factors and planting structure factor (represented by K_{cw}) to agricultural water demand (*AWD*) variations based on traditional attribution analysis ($Con_{Vi,r}$) and numerical experiments ($Con_{Vi,e}$)

		T_{max} case	T_{min} case	*uz* case	*n* case	RH_{max} case	RH_{min} case	K_{cw} case	Base case	Observation
1960–1988	$Con_{Vi,r}$ (%)	0.32	−0.26	−7.82	−1.90	−2.60	0.53	–	–	–
	$Trend_{AWD}$ (mm/year)	0.34	0.33	−1.59	−0.04	0.13	0.23	–	0.23	−2.76
	$Con_{Vi,e}$ (mm/year)	0.29	0.73	−7.01	−1.93	−1.79	0.12	–	–	–
1989–2015	$Con_{Vi,r}$ (%)	3.37	22.39	16.6	9.94	16.7	13.03	24.76	–	–
	$Trend_{AWD}$ (mm/yr)	0.75	0.73	1.45	0.86	0.62	0.71	7.10	0.54	9.47
	$Con_{Vi,e}$ (mm/yr)	0.95	3.14	4.76	2.71	2.69	2.99	26.91	–	–

contribution of each forcing factor was quantified using both traditional contribution analysis and numerical experiments approach.

Table 2 summarizes the *AWD* trends in the Tarim River Basin and their attributions. A substantial decrease (−2.76 mm/year) was seen during 1960–1988 while obvious increase (9.47 mm/year) during 1989–2015. For the traditional contribution analysis, *uz*, RH_{max} and *n* were detected to be the most important factors causing the decrease of *AWD* during 1960–1988 with the $Con_{Vi,r}$ (i.e. $S_{Vi} \times L \times Trend_{Vi}/|\overline{Vi}| \times 100$) being −7.82, −2.60 and −1.90%, respectively (Fig. 5). The contributions of *uz* computed by the traditional method ranged from −16.6 to −2.44%, with a mean value of −7.82% (Table 2).

For numerical experiment, the trend of *AWD* ($Trend_{AWD}$) of the *base case* (all meteorological factors and K_{cw} were detrended) was 0.23 mm/year during 1960–1988 and 0.54 mm/year during 1989–2015, equivalent to relative changes of 0.9 and 2.0%, respectively. The results confirmed that the new detrended time series can be practically regarded as the base case to be compared against the following numerical experiments (Zhang *et al.*, 2016). For period 1960–1988, T_{max} and T_{min} case resulted in average decrease rates for *AWDs* of 0.34 and 0.33 mm/year, respectively, comparable with that of the base case and indicating that T_{max} and T_{min} had negligible impact on *AWD*. The variation of *uz* alone was expected to lead to a dramatic decrease in *AWD*, with a decrease of 1.59 mm/year, which was recognized to be the dominant factor causing *AWD* decrease during 1960–1988. For the RH_{max} and RH_{min} case, RH_{max} and RH_{min} variations were suggested to cause decreases of 2.60 and 0.53 mm/year, respectively, in *AWD*. $Con_{Vi,e}$represented the effect of factor V_i to *AWD* variation base on the numerical experiments. $Con_{Tmax,e}$ (i.e., $(\delta AWD/\delta T_{max})(\delta T_{max}/\delta t)$) of the five states fell into the range of (–0.06, 0.68), with a mean value of 0.29 mm/year and an absolute mean value of 0.35 mm/year, indicating that T_{max} has a negligible positive effect on *AWD* (Fig. 6). For the T_{min} case, the $Con_{T_{min},e}$ values fell into the range (–1.04–2.81) with a mean value of 0.73 mm/year and an absolute mean value of 1.15 mm/year, which meant that the contribution of T_{min} to *AWD* was stronger than that of T_{max}. The most important factor influencing *AWD* variation was also recognized to be *uz*, with the mean value being −7.01 mm/yr, followed by *n* and RH_{max}. Meteorological factors, such as T_{max}, T_{min} and RH_{min} had much smaller impacts on *AWD* compared with *uz*, *n* and RH_{max}. The results were consistent with the findings based on the traditional analysis.

Figure 7*a* demonstrates basin-scale contributions of meteorological factors and K_{cw} to *AWD* variations. As K_{cw} was considered to remain unchanged during 1960–1988, this means that the

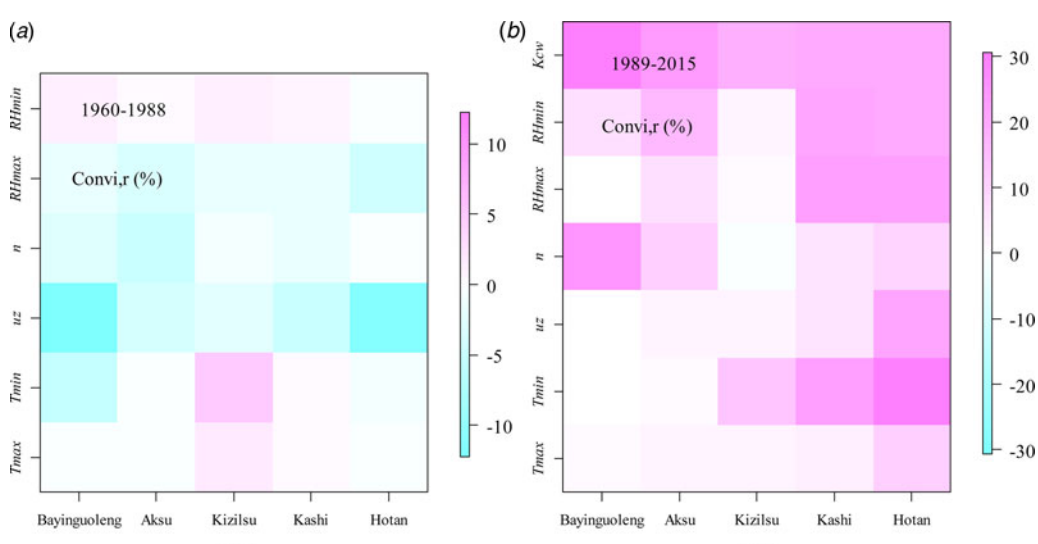

Fig. 5. State-scale contributions of the climate variables and human activities (measured by planting structure factor, K_{cw}) to agricultural water demand (*AWD*) variations based on the traditional analysis ($Con_{Vi,r}$) for period 1960–1988 (*a*) and 1989–2015 (*b*).

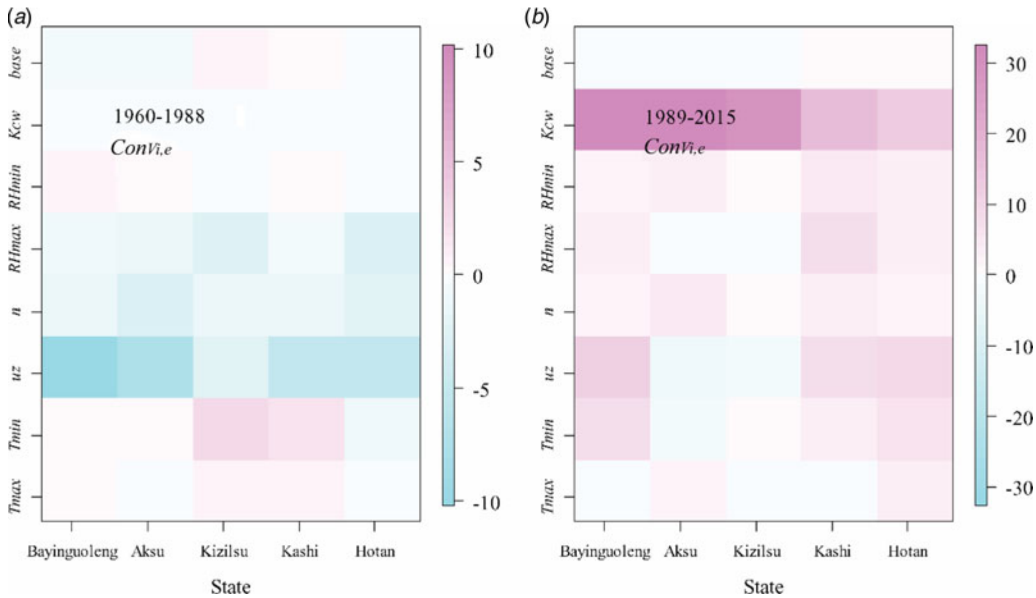

Fig. 6. State-scale contributions of climate variables and human activities (measured by planting structure factor, K_{cw}) to agricultural water demand (*AWD*) variations based on a series of numerical experiments ($Con_{Vi,e}$) for period 1960–1988 (*a*) and 1989–2015 (*b*). Each row indicated one experiment. T_{max} *case* (detrending all variables except for the maximum temperature); the T_{min} (minimum temperature) *case*; the *uz* (wind speed) *case*; the *n* (sunshine hours) *case*; the RH_{max} (maximum relative humidity) *case*; the RH_{min} (minimum relative humidity) *case*; the K_{cw} (planting structure factor, K_{cw}, factor) *case* and the *Base case* (detrending all forcing factors).

changes of observed *AWD* were caused merely by climate change. The impacts of climatic factors to *AWD* variation can be regarded as the differences between the observation (changing trend was −2.8 mm/year) and the base case (changing trend was −0.3 mm/year).

For the second period, 1989–2015, *AWD* increased dramatically with an average basin-scale increase rate of 9.47 mm/year. From the traditional contribution analysis, the variation of K_{cw} contributed 24.76% of the *AWD* increment, followed in a descending order by T_{min}, RH_{max}, *uz*, RH_{min}, *n* and T_{max} (Table 2). For all states, K_{cw} was the most prominent factor, with $Con_{Vi,r}$ ranging from 18.70 mm/year to −12.5 mm/year, but especially for Bayinguoleng (Fig. 4).

For the numerical experiment, if all meteorological factors were detrended, the trend in K_{cw} alone could result in an increase in *AWD* ($Trend_{AWD}$) with a rate of 7.10 mm/yr. For T_{max}, T_{min}, *uz*, *n*, RH_{max} and RH_{min}, these meteorological factors had much weaker effects on *AWD* variation with $Trend_{AWD}$ values ranging from 0.62 to 1.45 mm/year (Table 2). The *AWD* trends caused by each meteorological factor were comparable to those of the base case (0.54 mm/year, detrending all the forcing factors) (Fig. 5). $Con_{T_{max},e}$ (i.e. $(\delta \text{AWD}/\delta T_{max})(\delta T_{max}/\delta t)$ values) of the five states fell into the range of (−0.27,2.80), with the mean value being 0.95 mm/year and mean absolute value being 1.20 mm/year. $Con_{Vi,e}$ caused by *uz*, T_{min} and *n* were relatively higher, with the mean values being 4.76, 3.14 and 2.71 mm/year, respectively. The $Con_{Kcw,e}$ was estimated to be the highest, indicating that the influence of K_{cw} was the highest among all these forces. The increase in crop water requirement was caused mainly by the sharp increase in K_{cw} since 1989. The effects of forcing factors on *AWD* variation were comparable to each other based on traditional contribution analysis. However, in the

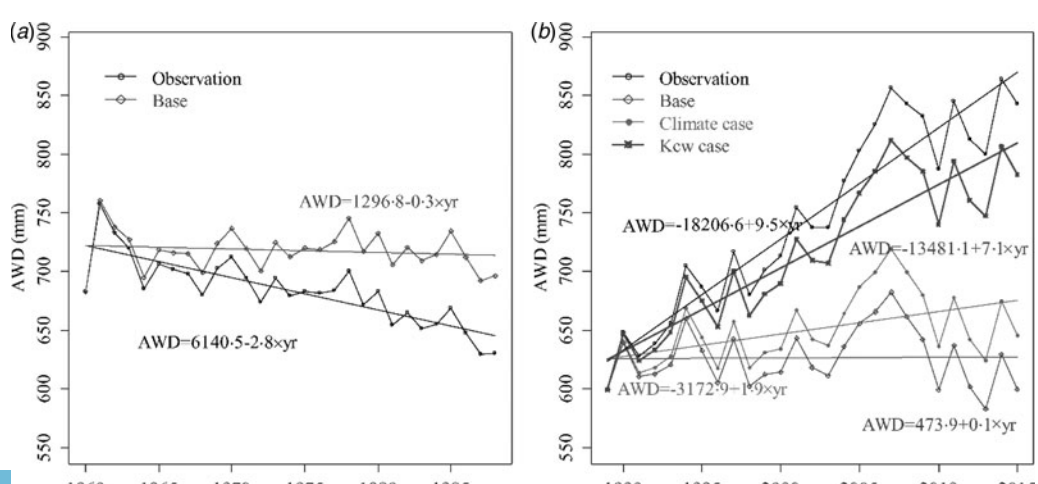

Fig. 7. Agricultural water demand (*AWD*) variations in the Tarim River Basin under different numerical experiments.

numerical experiment, the effect of K_{cw} was identified as the most pronomient (dominant) factor resulting to the *AWD* increase.

Figure 7*b* shows different patterns of *AWD* variation during 1989–2015. The most significant increase was evaluated to be the observation, which was due to the positive impacts of both climate change and evolution of planting structure. The variation of K_{cw} had a dominant effect on *AWD*, as the increment of *AWD* under the K_{cw} *case* was 7.1 mm/year, much higher than that of the climate case (i.e. keeping K_{cw} unchanged and keeping the original variations of meteorological factors) with increasing rate being 1.9 mm/year. The sharp increasing trend of observed *AWD* has turned to an apparent hiatus during 2008–2015, which was caused by the joint effects of both climate change (climatic variables did not show obvious trends) and human activity (K_{cw} kept stable).

Discussion

Contribution of meteorological factors to agricultural water demand

Understanding *AWD* change is key to developing irrigation strategies, improving water use efficiency and understanding hydrological, climatic and ecosystem processes. With global warming, actual evapotranspiration (reflecting agricultural water use) over land increased from the early 1980s up to the late 1990s on a global scale (Wild *et al*., 2008; IPCC 2013).

Many previous studies investigated variation of reference evapotranspiration and its response to climate change (Rodríguez Díaz *et al*., 2007; Mo *et al*., 2009; Shen *et al*., 2013; Fan *et al*., 2016). As argued by previous researches (Mo *et al*., 2009; Li *et al*., 2017*a*), *AWD* variation was also related to meteorological factors other than the six factors used in the current study, which should also be taken into account to estimate *AWD* accurately.

In the current study, the variations of *AWD* was examined over the arid Tarim River Basin. Based on previous studies (Li *et al*., 2014; Guo *et al*., 2015) and the current study, it was found that *AWD* decreased during 1960–1988 and then increased during 1989–2015. The contributions to the variation were analysed further. It was demonstrated that *uz* was the most prominent meteorological factor contributing to *AWD* variation during 1960–1988, which was consistent with those studies conducted in the arid north-west of China (Huo *et al*., 2013; Li *et al*., 2014), the humid Haihe River Basin (Mo *et al*., 2017), the arid Iran (Mosaedi *et al*., 2017), Spain (Rodríguez Díaz *et al*., 2007) and north-west Bangladesh (Acharjee *et al*., 2017).

Crop types influence *AWD* dramatically (Zwart and Bastiaanssen, 2004). If crop planting structure was not considered, the basin-scale *AWD* would still increase during 1989–2015, but with a much smaller slope (1.9 mm/year compared with the observed value of 9.47 mm/year). Evolution in crop structure could greatly promote the increase of *AWD*, which gives a strong signal that optimizing planting structure would be an effective water-saving strategy. As future climate change will affect the water balance of irrigated agriculture, farmers and irrigation managers could consider adapting to new scenarios by adjusting planting structure (Toureiro *et al*., 2017).

However, an obvious disadvantage of the current study was that the climate change induced changes in growing season length and phenological stages of crops were not considered. For example, a combination of beneficial carbon dioxide (CO_2) effects on plants, shorter growing periods and regional precipitation increases could lead to a decrease in global irrigation demand by ~17% (Konzmann *et al*., 2013). It has been stated that when temperature increases by 1 °C, it can be expected that the growing season will decrease by 2 days and the water requirement will increase by 1.4 for spring wheat in the arid Heihe River Basin (Han *et al*., 2017). For the humid coasts of the Caspian Sea in Iran, crop water requirement of maize is expected to increase by 10.6–15.3% in the future, despite an obvious reduction in the length of the growing season (Karandish *et al*., 2017).

Potential water risk in the Tarim River Basin

In the Tarim River Basin, runoff is generated in the high mountains, recharged by glacier/snow melt water and precipitation. The oases could hardly survive without irrigation. Even though runoff has increased slightly due to more meltwater and slightly increased precipitation with current warming (Fang *et al*., 2017), the increased area of irrigated land is consuming much more water than before. The water crisis is becoming more and more prominent, especially for some critical water-demanding periods, i.e. April, May and even June in some specific arable lands. This kind of seasonal water shortage reinforces water stress in the study region. As shown in the current study, the large proportion of high-water-consuming crops together with the unprecedented enlargement of crop growing area has resulted in a rapid increase in crop water demand. It has also already caused ecological degradation in the lower reaches of the Tarim River (Shen and Chen, 2010; Shen *et al*., 2013), such as the shrinkage of terminal lakes and the drying up of rivers (Chen *et al*., 2011). Even though the Chinese government has put 10.7 billion RMB into implementing water-saving projects and guaranteeing water going downstream, serious problems (e.g. with improved canal water use efficiency, more and more land have been excessively, illegally cultivated) should also be recognized.

In addition, with further warming, glacier runoff will reach a peak in the coming years and the Shiyang River (Zhang et al., 2015) will have less water in summer months (Fang *et al*., 2017). The Tarim River Basin, the most important area for cotton and grain production, supports a population of 11 million people (Deng, 2016). Therefore, it is urgent to implement water management such as regulation on water price and adjustment of crop planting structure, as well as water-saving technologies in this hyper-arid region, to cope with the ever more serious water crisis.

Conclusions

Agricultural water consumption, accounting for 95% of total water use in the Tarim River Basin, is the main factor affecting water resource allocation. Based on the Penman–Monteith equation and crop coefficient approach, crop water requirement since 1960 was estimated and the contributions of meteorological factors and planting structure to *AWD* variation were quantified. The following conclusions can be drawn:

(1) *AWD* experienced a decreasing trend during 1960–1988 with a rate of −2.76 mm/year; but then increased from 1989 at a very high rate of 9.47 mm/year.
(2) Wind speed and sunshine hours decreased over the period 1960–1988 and then increased from 1989–2015. The

proportions of planting area of high water-consuming crops (e.g. cotton, fruit trees) have increased.

(3) The traditional contribution analysis method and the numerical experiment approach generated consistent results. For 1960–1988, the most significant factor inducing *AWD* variation was wind speed (*uz*), followed by RH_{max} and sunshine duration (*n*); other meteorological factors were not as important as these three. For 1989–2015, the dominant factor affecting *AWD* was K_{cw} (representing the weighted K_c values caused by the evolution of planting structure). The application of two different contribution analysis methods could provide robust results and these conclusions will shed light on detecting effective approaches for future water-saving strategies.

Financial support. This work was supported by the CAS 'Light of West China' Program (grant no. 2016-QNXZ-B-12), the National Natural Science Foundation of China (grant no. 41701043) and the Strategic Priority Research Program of Chinese Academy of Sciences (grant no. XDA20100300).

Conflicts of interest. None.

Ethical standards. Not applicable.

References

Acharjee TK *et al.* (2017) Declining trends of water requirements of dry season Boro rice in the north-west Bangladesh. *Agricultural Water Management* **180**, 148–159.

Allen RG *et al.* (1998) *Crop Evapotranspiration – Guidelines for Computing Crop Water Requirements*. FAO Irrigation and drainage paper No. 56. Rome, Italy: FAO.

Allen RG *et al.* (2005) FAO-56 dual crop coefficient method for estimating evaporation from soil and application extensions. *Journal of Irrigation and Drainage Engineering* **131**, 2–13.

Calera A *et al.* (2017) Remote sensing for crop water management: from ET modelling to services for the end users. *Sensors* **17**, E1104.

Chen Y (2015) *Ecological Protection and Sustainable Management of the Tarim River Basin*. Beijing, China: Science Press.

Chen Y, Ye Z and Shen Y (2011) Desiccation of the Tarim river, Xinjiang, China, and mitigation strategy. *Quaternary International* **244**, 264–271.

Chen F *et al.* (2009) Rapid warming in mid-latitude Central Asia for the past 100 years. *Frontiers of Earth Science in China* **3**, 42. https://doi.org/10.1007/s11707-009-0013-9.

Chen Y *et al.* (2016) Water and ecological security: dealing with hydroclimatic challenges at the heart of China's silk road. *Environmental Earth Sciences* **75**, 881. https://doi.org/10.1007/s12665-016-5385-z.

Chen X *et al.* (2017) Ecological effect evaluation of comprehensive control project in Tarim River Basin. *Bulletin of Chinese Academy of Sciences* **32**, 20–28.

Deng M (2016) Prospecting development of south Xinjiang: water strategy and problem of Tarim River Basin. *Arid Land Geography* **39**, 1–11.

Döll P (2002) Impact of climate change and variability on irrigation requirements: a global perspective. *Climatic Change* **54**, 269–293.

Fan J *et al.* (2016) Climate change effects on reference crop evapotranspiration across different climatic zones of China during 1956–2015. *Journal of Hydrology* **542**, 923–937.

Fang G *et al.* (2017) Impact of GCM structure uncertainty on hydrological processes in an arid area of China. *Hydrology Research*, nh2017227. Doi: 10.2166/nh.2017.227.

Guo D, Westra S and Maier HR (2016) An R package for modelling actual, potential and reference evapotranspiration. *Environmental Modelling & Software* **78**, 216–224.

Gao G *et al.* (2006) Spatial and temporal variations and controlling factors of potential evapotranspiration in China 1956–2000. *Journal of Geographical Sciences* **16**, 3–12.

Guo B *et al.* (2015) Risk assessment of regional irrigation water demand and supply in an arid inland river basin of northwestern China. *Sustainability* **7**, 12958–12973.

Han DM *et al.* (2017) Effects of climate change on spring wheat phenophase and water requirement in Heihe River Basin, China. *Journal of Earth System Science* **126**, 9.

Huo Z *et al.* (2013) Effect of climate change on reference evapotranspiration and aridity index in arid region of China. *Journal of Hydrology* **492**, 24–34.

IPCC (2013) *Climate Change 2013 – The Physical Science Basis*. Working Group I Contribution to the Fifth Assessment Report of the Intergovernmental Panel on Climate Change. Cambridge and New York: Cambridge University Press.

Karandish F, Kalanaki M and Saberali SF (2017) Projected impacts of global warming on cropping calendar and water requirement of maize in a humid climate. *Archives of Agronomy and Soil Science* **63**, 1–13.

Konzmann M, Gerten D and Heinke J (2013) Climate impacts on global irrigation requirements under 19 GCMs, simulated with a vegetation and hydrology model. *Hydrological Sciences Journal* **58**, 88–105.

Li Z *et al.* (2014) Potential evapotranspiration and its attribution over the past 50 years in the arid region of northwest China. *Hydrological Processes* **28**, 1025–1031.

Li C *et al.* (2017*a*) Spatial and temporal evolution of climatic factors and its impacts on potential evapotranspiration in loess plateau of northern Shaanxi, China. *Science of the Total Environment* **589**, 165–172.

Li Z *et al.* (2017*b*) Multivariate assessment and attribution of droughts in Central Asia. *Scientific Reports* **7**, 1316.

Liang L, Li L and Liu Q (2011) Spatio-temporal variations of reference crop evapotranspiration and pan evaporation in the west Songnen plain of China. *Hydrological Sciences Journal* **56**, 1300–1313.

Liu B *et al.* (2004) Taking China's temperature: daily range, warming trends, and regional variations, 1955–2000. *Journal of Climate* **17**, 4453–4462.

McCuen RH (1974) A sensitivity and error analysis CF procedures used for estimating evapotration. *JAWRA Journal of the American Water Resources Association* **10**, 486–497.

McMahon TA *et al.* (2013) Estimating actual, potential, reference crop and pan evaporation using standard meteorological data: a pragmatic synthesis. *Hydrology and Earth System Sciences* **17**, 1331–1363.

Mo X *et al.* (2009) Regional crop yield, water consumption and water use efficiency and their responses to climate change in the north China plain. *Agriculture, Ecosystems & Environment* **134**, 67–78.

Mo X *et al.* (2017) Sensitivity of terrestrial water and carbon fluxes to climate variability in semi-humid basins of Haihe River, China. *Ecological Modelling* **353**, 117–128.

Mosaedi A *et al.* (2017) Sensitivity analysis of monthly reference crop evapotranspiration trends in Iran: a qualitative approach. *Theoretical and Applied Climatology* **128**, 857–873.

Rodríguez Díaz JA *et al.* (2007) Climate change impacts on irrigation water requirements in the Guadalquivir river basin in Spain. *Regional Environmental Change* **7**, 149–159.

Sen PK (1968) Estimates of the regression coefficient based on Kendall's tau. *Journal of the American Statistical Association* **63**, 1379–1389.

Shen Y and Chen Y (2010) Global perspective on hydrology, water balance, and water resources management in arid basins. *Hydrological Processes* **24**, 129–135.

Shen Y *et al.* (2013) Estimation of regional irrigation water requirement and water supply risk in the arid region of northwestern China 1989–2010. *Agricultural Water Management* **128**, 55–64.

Sherwood S and Fu Q (2014) A drier future? *Science* **343**, 737–739.

Statistical Bureau of Xinjiang Uygur Autonomous Region (1989–2016) *Xinjiang Statistical Yearbooks*. Beijing, China: China Statistics Press. Available at http://tongji.cnki.net/overseas/engnavi/YearBook.aspx?id=N2011100020&floor=1 (Accessed 4 April 2018).

Tabari H and Talaee PH (2014) Sensitivity of evapotranspiration to climatic change in different climates. *Global and Planetary Change* **115**, 16–23.

Toureiro C *et al.* (2017) Irrigation management with remote sensing: evaluating irrigation requirement for maize under Mediterranean climate condition. *Agricultural Water Management* **184**, 211–220.

Wang Z *et al.* (2015) Jujube drip irrigation water consumption and its crop coefficient in oasis of arid areas. *Xinjiang Agricultural Sciences* **52**, 675–680, [In Chinese with English Abstract].

Wild M, Grieser J and Schär C (2008) Combined surface solar brightening and increasing greenhouse effect support recent intensification of the global land-based hydrological cycle. *Geophysical Research Letters* **35**, L17706. https://doi.org/10.1029/2008GL034842.

Yin Y *et al.* (2008) Radiation calibration of FAO56 Penman-Monteith model to estimate reference crop evapotranspiration in China. *Agricultural Water Management* **95**, 77–84.

Zhai P *et al.* (2005) Trends in total precipitation and frequency of daily precipitation extremes over China. *Journal of Climate* **18**, 1096–1108.

Zhang S, Gao X and Zhang X (2015) Glacial runoff likely reached peak in the mountainous areas of the Shiyang River Basin, China. *Journal of Mountain Science* **12**, 382–395.

Zhang L, Zhang N and Ma Y (2010) Study on water use of walnut trees under drip irrigation. *Modern Agricultural Sciences and Technology* **2010–21**, 117–121, [In Chinese with English Abstract].

Zhang J *et al.* (2016) Dependence of trends in and sensitivity of drought over China (1961–2013) on potential evaporation model. *Geophysical Research Letters* **43**, 206–213.

Zwart SJ and Bastiaanssen WGM (2004) Review of measured crop water productivity values for irrigated wheat, rice, cotton and maize. *Agricultural Water Management* **69**, 115–133.